

A Point-Placement Strategy for Conforming Delaunay Tetrahedralization*

Michael Murphy[†] David M. Mount[‡] Carl W. Gable[§]

Abstract

A strategy is presented to find a set of points which yields a Conforming Delaunay tetrahedralization of a three-dimensional Piecewise-Linear Complex (PLC). This algorithm is novel because it imposes no angle restrictions on the input PLC. In the process, an algorithm is described that computes a planar conforming Delaunay triangulation of a Planar Straight-Line Graph (PSLG) such that each triangle has a bounded circumradius, which may be of independent interest.

1 Introduction

In many two- and three-dimensional geometric modeling problems, notably the numerical approximation of the solution to a Partial Differential Equation with a Finite-Element type method [SF73], it is very desirable to obtain a triangulation (tetrahedralization) that respects the domain of interest. The task of forming such decompositions, along with ensuring that the elements of the decompositions satisfy application-specific quality requirements, is sometimes referred to as unstructured mesh generation. See [BE92] for a survey. The Delaunay triangulation, a celebrated structure in Computational Geometry, can play a central role in this process [GB98] [She98b] due to many important geometric properties and the existence of efficient algorithms to compute and maintain one with a dynamic set of points. (We shall assume the reader is familiar with the Delaunay triangulation and its basic properties, notably the “empty-circle” characterization; see [PS85] for a definition, a discussion of its properties, and algorithms for computing and maintaining the Delaunay triangulation.) Adapting the Delaunay triangulation, defined over point sets, to more complicated geometric domains such as arbitrary polygons or polyhedra, has proven to be a major challenge of unstructured mesh generation. To cope, researchers have developed the *Constrained Delaunay triangulation*, which changes the “empty-circle” criterion based on the domain. Another adaptation is the *Conforming Delaunay triangulation*, which is obtained when the domain is respected by the Delaunay triangulation of a set of representative points. Thus, to obtain a conforming Delaunay triangulation of a domain, the resolution typically must be increased through the addition of points, often called

*A preliminary version of this paper appeared in the *Proc. 11th Annual ACM-SIAM Symp. on Discrete Algorithms*, 2000, 67–74.

[†]Department of Computer Science, University of Maryland—College Park and Los Alamos National Laboratory. Email: murphy@cs.umd.edu.

[‡]Department of Computer Science and Inst. for Advanced Computer Studies, University of Maryland—College Park. Email: mount@cs.umd.edu. This author was supported by the National Science Foundation under grant CCR-9712379.

[§]Geoanalysis Group, Earth and Environmental Science Division, Los Alamos National Laboratory. Email: gable@lanl.gov.

Steiner points. In the plane, these structures are well-understood and efficient algorithms to work with them exist. However, the analogs of these structures in three and higher dimensions pose many algorithmic challenges. In this paper, we address part of the challenges of three-dimensional unstructured mesh generation by giving a provably correct algorithm to construct a Conforming Delaunay tetrahedralization.

1.1 Piecewise-linear representations

We start by elaborating upon what we mean by a domain. We shall concentrate on piecewise-linear representations. Polygons and polyhedra fall into this class. However, for problems involving multiply-connected boundaries, they are not expressive enough. For example, in a geological application, one may need to represent several layers of rocks, each having unique material properties that need to be distinguished in the simulation. The boundaries between rock layers, the *material interfaces*, may be very complicated, especially if there are cracks and faults present. For such demanding applications, the most general class of two-dimensional piecewise-linear representations, the *Planar Straight Line Graph* (PSLG), (see *e.g.* [PS85]) which encompasses polygons, polygons with holes, and all other planar, piecewise-linear, multi-material representations, is needed. PSLGs consist of vertices and line segments, also referred to as edges. Vertices are specified by providing the coordinates. Line segments are specified by giving the connections between vertices; the line segments must be non-overlapping, except when meeting at a common vertex. In three dimensions the *Piecewise-Linear Complex* (PLC) class (using the notation of [MTT⁺96] and [She98b]) is the most general representation. In the PLC model, the objects consist of vertices, line segments, and planar faces, possibly with holes and slits. An equivalent formulation of a PLC as well as the “Radial-Edge” data structure to represent one are given in [Wei87].

1.2 Conforming Delaunay triangulations

We return to the problem of adapting Delaunay triangulations to piecewise-linear domains. One adaptation, the *Constrained Delaunay triangulation*, relaxes the “empty-circle” property. A formal definition, and a $\Theta(n \log n)$ algorithm to compute one in the plane is given in [Che89a]. Although in three dimensions, there is no immediate generalization of the Constrained Delaunay triangulation, a structure known as the “Conforming-Constrained” Delaunay tetrahedralization is defined in [She98a]. However, it should be noted that Constrained and Conforming-constrained Delaunay triangulations and tetrahedralizations are not as helpful with some numerical schemes because the quality requirements imposed on internal boundaries (material interfaces) imply that triangles incident upon these edges are “locally Delaunay.” Specifically, for an internal edge in a PSLG, P , some schemes require that the two angles opposite that edge in the triangulation of P be nonobtuse.

Therefore, although the Constrained Delaunay triangulation requires no Steiner points to obtain and the Constrained-Conforming Delaunay tetrahedralization may require fewer Steiner points, algorithms to compute Conforming Delaunay triangulations and tetrahedralizations are of great interest in unstructured mesh generation. To obtain a Conforming Delaunay triangulation of a PSLG, P , one places Steiner points to ensure that all of the edges of P are represented in the Delaunay triangulation of the original point set together with the Steiner points. For this purpose, Steiner points never need to be placed anywhere but on the edges of the PSLG; this is often referred to as *edge refinement*. The sufficiency of edge refinement is a consequence of the following standard lemma (see *e.g.* [She98a]):

LEMMA 1.1. *An edge e of a PSLG P with vertex set V is an edge of the Delaunay triangulation of V if and only if there exists a circle passing through the vertices of e containing no points of V in*

its interior.

Saalfeld’s algorithm [Saa91] for computing a Conforming Delaunay triangulation of a PSLG is based directly upon Lemma 1.1. To see the intuition, imagine for the moment that we have a PSLG, P , that consists of completely disjoint line segments. (That is, only one line segment is incident upon a vertex.) One strategy to satisfy Lemma 1.1 in this special case is to compute the closest distance between two segments $d_{min} > 0$. Next, pack a set of circles centered on every edge e with a radius no larger than d_{min} so that two adjacent circles in the packing are tangent upon their points of intersection with e . Steiner points can then be placed on e at these points of tangency, as shown in Figure 1(b). This strategy decomposes each edge of P into smaller edges, each of which satisfies Lemma 1.1 because the disks covering e cannot contain a point on another edge. Thus, we have a conforming Delaunay triangulation. Of course, many edges of a PSLG can be incident on a common vertex. Hence, the first phase of Saalfeld’s algorithm is to guard every vertex v by placing a sufficiently small disk centered around v so that the disk does not intersect any edge not incident upon v . Steiner points are placed at the intersection of this disk with the edges of v . As shown in Figure 1(a), the minimum diameter circle passing through the portion of each edge from v to these Steiner points will be empty, satisfying Lemma 1.1. After this step, what remains is in essence a set of disjoint edges that can be processed in the manner just described.

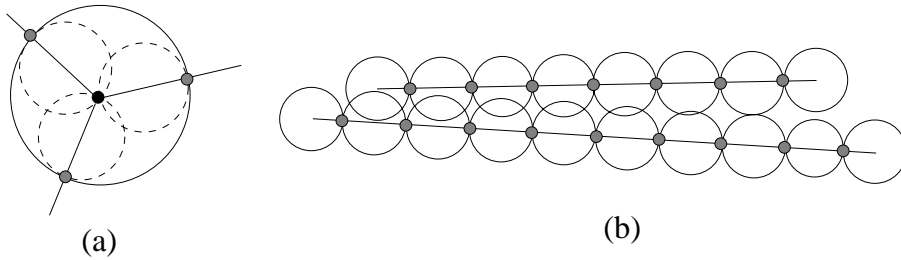


Figure 1: Key steps in Saalfeld’s Conforming Delaunay triangulation algorithm. **(a)**: Protecting the vertices. **(b)**: Covering the edges with empty tangent circles.

Because it can place an excessive number of Steiner points, Saalfeld’s algorithm should be viewed more as a simple existence proof of a Conforming Delaunay triangulation than as a practical algorithm. There are at least two noteworthy provably correct algorithms to find a Conforming Delaunay triangulation of a PSLG that are sensitive to the number of Steiner points. The first is Edelsbrunner and Tan’s algorithm [ET93], which gives a striking $O(n^3)$ combinatorial upper bound on the number of Steiner points placed, where n is the input size. The other is Ruppert’s Delaunay-Refinement algorithm [Rup95] using “the Quitter” given in [She97] to resolve small input angles. Although the latter algorithm does not admit combinatorial bounds on the number of Steiner points placed – the bounds come from the local-feature-size, an intrinsic geometric property of the domain – Ruppert’s algorithm is quite practical and can be used to construct a no-small-angle triangulation, useful in bounding discretization error in the Finite-Element method.

1.3 A strategy for conforming Delaunay tetrahedralization

Many heuristic, or at least unproven, algorithms can be found in the literature to successfully compute a Conforming Delaunay tetrahedralization. See for example, [HKM95]. However, a provably correct algorithm for computing a Conforming Delaunay tetrahedralization of a general PLC is apparently an open problem [BP97] [CDE⁺99] [CM99] [Geo99] [Bak99]. Some provably

correct algorithms to find a conforming Delaunay tetrahedralization make stringent angle restrictions on the input PLC [She98b] [MTT+96]. To be sure, these algorithms were designed to provide “quality” Delaunay tetrahedralizations, where a bounded ratio of circumradius to shortest edge of each tetrahedron is the measure of interest, rather than any Delaunay tetrahedralization. However, unlike Ruppert’s planar algorithm, which has a similar motivation and makes similar angle restrictions that can be side-stepped, these restrictions are not as readily resolved. Our purpose is to give an algorithm to find a Conforming Delaunay triangulation of a PLC with no angle restrictions, a step towards both practical and provably correct Delaunay-based mesh generation in three dimensions.

The problem in three dimensions is more involved because both edges *and* faces of a PLC must be refined until they are part of the Delaunay tetrahedralization of the augmented point set. The three-dimensional analog of Lemma 1.1 for edges in a PLC not part of any face remains the same except that we require empty spheres rather than circles. A straightforward generalization of Saalfeld’s algorithm can be used to process these edges. Therefore, such hanging edges are considered no further. Rather, we are concerned with refining the faces. The analog of Lemma 1.1 becomes:

LEMMA 1.2. *A triangular face f (or a face with four or more cocircular vertices) of a PLC P with vertex set V is a face in the Delaunay tetrahedralization of V if and only if there exists a sphere passing through the vertices of f containing no points of V in its interior.*

If the face is not triangular, then the planar Delaunay triangulation of the vertices of the face must be conforming with each triangle (face with four or more cocircular vertices) must satisfy Lemma 1.2.

The algorithm we describe is motivated by the following observation: Suppose we are given a set of disjoint faces in \mathbb{R}^3 which we wish to refine so that the Delaunay tetrahedralization of the augmented point set conforms to these faces. A sufficient but not necessary condition is to find a *planar* Delaunay triangulation of each face with the property that for each triangle, t , the circumscribing sphere of radius equal to the radius of the (planar) circumcircle of t does not intersect any other face. Note that this sphere is the one of minimum radius circumscribing t . A planar conforming Delaunay triangulation of each face where each triangle has a radius bounded by the distance to the nearest face in the PLC will satisfy this condition. We give an adaptation of Chew’s guaranteed-quality Delaunay triangulation algorithm [Che89b] for this purpose in Section 2.

Of course, the faces need not be disjoint. As a consequence, the above strategy fails because the distance between two incident faces is zero. However, methods used in our adaptation of Chew’s algorithm to protect vertices and edges extend to three dimensions. What remains after these protection phases is a set of disjoint subfaces upon which we can use our bounded circumradius conforming Delaunay triangulation algorithm. We show that the results of the protection phases and the planar triangulation phases do not interfere. Thus, we have a refinement of the PLC such that a Conforming Delaunay tetrahedralization can be obtained from its vertices.

2 Delaunay triangulations with bounded circumradii

We proceed by finding a conforming Delaunay triangulation of a PSLG such that the circumradius of each triangle is bounded from above by a pre-specified constant. One early guaranteed-quality Delaunay triangulation algorithm due to Chew [Che89b] shows promise. Although the intention of his algorithm is to produce a Constrained Delaunay triangulation such that the angles in the triangulation are between 30 and 120 degrees, it also generates triangles with bounded circumradii. However, before applying his algorithm to our task, two problems need to be addressed. First, the precondition of his algorithm requires that no input angle can be less than 30 degrees. Second, his

algorithm does not guarantee a Conforming Delaunay triangulation, only a Constrained Delaunay triangulation. We present modifications that address both issues while maintaining the user-specified upper bound on the largest circumradius.

2.1 Review of Chew’s algorithm

Chew’s algorithm takes as input a PSLG P such that no angle incident upon a vertex is less than 30 degrees and a parameter r_{max} from the user. The output is a Constrained Delaunay triangulation such that the circumradius of each triangle does not exceed r_{max} . The first step of his algorithm refines the edges of P into subsegments whose lengths are in the range $[h, \sqrt{3}h]$ for some $h \leq r_{max}$. The parameter h must be chosen small enough so that such a refinement is possible and so that h is no larger than the closest distance between any two (Steiner or input) vertices. Because of the precondition on the smallest angle, such a value always exists. (A general strategy for finding such an edge partition is given below.) After computing the Constrained Delaunay triangulation of the modified PSLG, circumcenters of triangles whose radii are larger than h are inserted, one at a time. The Constrained Delaunay triangulation can be restored after each such Steiner point insertion using Lawson’s algorithm [Law77]. The process continues until no triangles with circumradii exceeding h exist, which Chew demonstrates always occurs eventually.

2.2 Treating the small angles

If the input PSLG contains angles less than 30 degrees, finding a value for h so that the PSLG is decomposed into edges of length in the range $[h, \sqrt{3}h]$ and so that no two vertices are of distance less than h is impossible. However, such a decomposition is motivated more by the desire to avoid small angles than to prevent triangles with large circumradii. Although we use these length bounds in our proof, we can tolerate small angles by transforming small-angled PSLGs to ones Chew’s algorithm can process by adding a vertex-protection phase, resembling Saalfeld’s, prior to invoking Chew’s algorithm. We describe this phase in conjunction with the initial edge-refinement process.

Consider a PSLG P . Let δ be the minimum distance either between any two vertices or between a vertex and any non-incident edge. Let ϕ be the minimum of $\pi/4$ and the angle between two edges that share a vertex. Let $r = \delta/3$, and let h be any quantity that is no greater than the length of a chord of a circle of radius r subtending an angle of $\phi/2$. (By the law of cosines, $h \leq r\sqrt{2(1 - \cos(\phi/2))}$.) Because $\phi \leq \pi/4$, it is easy to verify that $h \leq r/2$.

As in Saalfeld’s vertex-protection phase, each vertex is surrounded by a protecting circle of radius r . Steiner points are placed at the intersection of each circle with the edges of P . This subdivides each circle into a collection of arcs of angular sizes at least ϕ . Each arc of angle θ is further subdivided into $k = \lfloor 2\theta/\phi \rfloor$ subarcs of equal sizes. Of course, if the subarc is outside the external boundary, we do not need to refine it. Steiner points are placed at the endpoints of these intervals. By connecting consecutive Steiner points, we form a convex polygon surrounding each input vertex. We connect the central vertex to these points by a set of “spokes,” forming a set of isosceles triangles. This is illustrated in Figure 2 for an internal vertex in the domain.

We assert that the distances between consecutive Steiner points on the circle are in the interval $[h, \sqrt{3}h]$. This is true because $\theta \geq \phi$ implies that $k \geq 2$. Combining this and the definition of k we have

$$\begin{aligned} \frac{k\phi}{2} &\leq \theta < \frac{(k+1)\phi}{2} \\ \frac{\phi}{2} &\leq \frac{\theta}{k} < \frac{(k+1)\phi}{2k} \end{aligned}$$

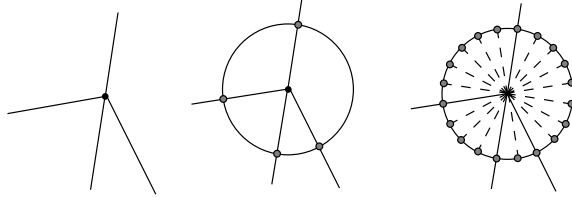


Figure 2: A vertex of a PSLG is protected by a circle of appropriate radius. Intersection points are added, and Steiner points are placed on the circle to satisfy Chew's point-spacing criteria.

$$\frac{\phi}{2} \leq \frac{\theta}{k} < \frac{3\phi}{4} < \sqrt{3}\frac{\phi}{2}.$$

Each subarc is of angular size θ/k . Two points subtending a subarc of angle $\phi/2$ are at distance h apart and two points subtending a subarc of $\sqrt{3}\phi/2$ are at most distance $h\sqrt{3}$ apart, as desired.

As we have just seen, the angles between consecutive spokes is less than $3\phi/4 < \pi/3$. Consider any isosceles triangle whose base is of length b and whose opposite angle at most $\pi/3$. It is straightforward to show that its circumcircle extends a distance at most $b/(2\sqrt{3})$ beyond the base. Since $b \leq \sqrt{3}h$, the circumcircles from this part of the construction do not extend a distance more than $h/2$ outside of the surrounding convex polygon. We use this fact later.

Observe that no two non-incident pairs (vertex-vertex or vertex-edge) can be closer than distance $3r$, implying that even after adding the surrounding circles of radius r , all non-incident entities are separated by a distance of at least $r > 2h$.

We create a new PSLG P' to be supplied to Chew's algorithm by adding the convex polygon surrounding each vertex to the PSLG and throwing out everything in its interior. The remaining edges are of length at least r (the minimum distance between circles). Each such edge of length l is subdivided into $j = \lfloor l/h \rfloor$ subsegments of equal lengths and Steiner points are placed at the endpoints of each subsegment. As noted earlier, $h/2 \leq r \leq l$, implying that $j \geq 2$. By the same argument above, it follows that the length of each subsegment is in the interval $[h, h\sqrt{3}]$. Because no two consecutive vertices are closer than h , and no two non-incident entities are closer than $2h$, it follows that no two vertices of this construction are closer than h . Thus, we can apply Chew's algorithm to the result.

We claim that after applying Chew's algorithm, the spokes joining each vertex of P to its surrounding convex polygon and the triangles created by Chew's algorithm with edges incident upon this polygon are "locally Delaunay." The reason is that Chew's algorithm does not place any vertices within distance $h/2$ of the boundary of the protecting polygons. By the observation made earlier, the circumcircles defined by these isosceles triangles do not extend outside of the convex polygon by a distance more than $h/2$. Thus Chew's triangles are protected from the circumcircles of the "spoke triangles." As a check, the circumcircles generated by Chew's algorithm do not penetrate the protecting polygon by a distance of more than $3h/2$ and therefore cannot contain the vertex that is being protected by the polygon. Thus, the spokes and Chew's triangles do not interfere with each other.

2.3 Protecting the input edges

Running the above vertex-protection scheme followed by Chew's algorithm on the modified PSLG P' will not necessarily yield a Conforming Delaunay triangulation. This is because for a segment of an edge e of P outside the vertex-protectors, the two angles of the triangles opposite to e can be obtuse,

violating the “empty-circle” condition (although they are “Constrained Delaunay.”) To remedy this, we shield each edge e from the circumcircles of triangles generated by Chew’s algorithm. The buffer-zones are formed by extruding parallel edges from e a distance d_e . This distance can be computed in the same manner h is computed in Section 2.2. If e is an internal edge, we extrude protectors on both sides of e . If e is a boundary edge, we only extrude into the domain. The intuition is that we will run Chew’s algorithm on the extruded edges rather than on e , leaving the space between e and its protectors as a buffer-zone to be triangulated separately. Although triangles generated by Chew’s algorithm can have circumcircles that intersect e , we can ensure that e is refined so that no Steiner point falls in the interior of these circles. To accomplish this, when refining these edges to satisfy Chew’s length conditions, it is important to obtain a sequence of identical intervals. We then refine e in exactly the same manner as its protectors. This alignment of Steiner points is shown in Figure 3.

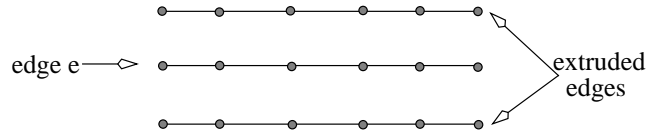


Figure 3: Two parallel edges are extruded from e and are refined with the same point distribution.

How do we incorporate these protecting edges with the vertex-protection phase just described? Rather than placing Steiner points at the intersection of the protecting circle and e , we place a Steiner point on the circle a vertical distance d_e above e , a Steiner point on the circle a distance d_e below e , and a Steiner point at their orthogonal projections onto e . We form the protecting edges parallel to e by connecting these Steiner points above and below e to their counterparts on the circle protecting the adjacent vertex. We consider the buffer-zone of a face to be anything inside the protecting circle or within a distance d_e of the edge on the face. The arcs outside the buffer-zone and the edge-protectors are divided to satisfy the spacing requirements of Chew’s algorithm using a value of h derived from this new PSLG. Note that the closest pair of points distance can now be smaller than before. Thus, $d_e \geq h$.

The input to Chew’s algorithm is the union of all of the protecting edges, as illustrated in Figure 4(c). Figure 4(d) shows what the triangulation of the buffer-zone looks like. As explained above, the spoke triangles are locally Delaunay. The circumcenters of triangles incident upon Steiner points placed on e can only extend a distance $h/2$, outside of the protected region. This is because of the spacing constraints imposed by Chew’s algorithm. Specifically, the circumcircle of a $\sqrt{3}h$ by d_e box can only bulge a distance $h/2$ outside of the the buffer-zone. This occurs when $d_e = h$. Thus, five co-circular points could exist in the worst case when Chew’s algorithm places a point a distance of $h/2$ of an edge of length $\sqrt{3}h$.

We now have the following theorem:

THEOREM 2.1. *A PSLG can be refined so that a Conforming Delaunay triangulation is obtained with the property that the circumradii of each Delaunay triangle is bounded from above by a pre-specified constant using a finite number of Steiner points.*

3 Extending to three dimensions

3.1 Overview

We extend the above algorithm to find a Conforming Delaunay tetrahedralization of a PLC, P . Like

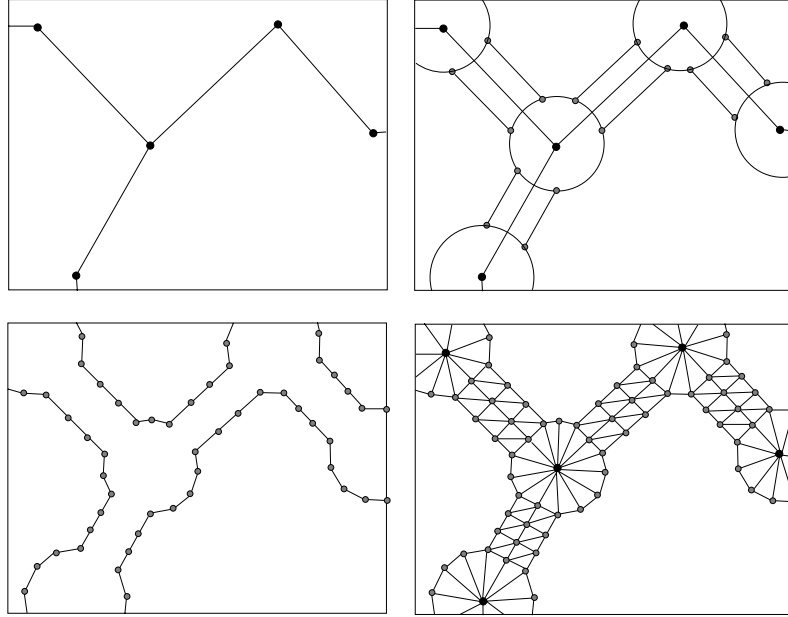


Figure 4: **(a)** A portion of a PSLG **(b)** Finding protecting circles and edges. **(c)** The PSLG passed to Chew’s algorithm to triangulate everything outside the buffer-zones. **(d)** The triangulation of the interior of the buffer-zone.

the two-dimensional algorithm, we create buffer-zones around the shared vertices and edges of faces. We then use Chew’s algorithm to create a (planar) conforming Delaunay triangulation of the portions of the faces outside the buffer-zones such that the minimum diameter sphere of every triangle in these triangulations cannot intersect another planar face outside a buffer-zone. This is illustrated in Figure 5. This satisfies Lemma 2 for each triangle if the buffer zones do not contain points where these spheres intersect. Again, the crux is to define the buffer-zones and refine them into triangles so that they do not interfere with the triangles produced by Chew’s algorithm. Fortunately, the vertex and edge protection methods of our planar bounded radius conforming Delaunay triangulation algorithm given above extend easily into three dimensions. The intuition behind the extensions is that when we protect shared vertices of P , we use protecting spheres centered at these vertices rather than protecting circles. To protect edges, we place protecting cylinders around them. However, the phrases “protecting spheres” and “protecting cylinders” are not entirely accurate because it is acceptable for a Delaunay edge to pierce these spheres and cylinders in the final tetrahedralization of the point set, if the piercing edge does not cross a face of P .

3.2 Creating the buffer-zones

The first step is to compute the size of the buffer-zones. The values of d_e and r defined above can be used for this purpose. The only difference in their computation is that we use as our δ the minimum distance between any two adjacent vertices or any two non-incident entities (vertex-vertex vertex-edge, vertex-face, edge-edge, edge-face, face-face). To avoid problems with ambiguities caused by two incident faces that pass close to each other far from the points of incidence (as can occur with non-convex faces), assume all faces are triangulated arbitrarily. We do not take into account dihedral angles at this point.

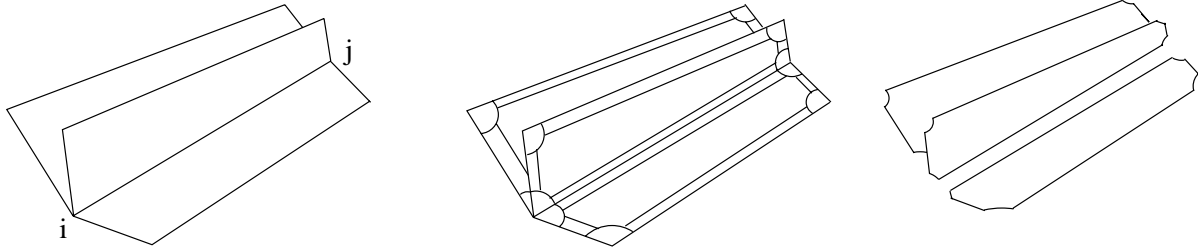


Figure 5: **(a)** Edge (i, j) has three faces incident upon it. **(b)** The buffer zones on each face formed by vertex-protection and edge-extrusion. **(c)** The disjoint faces passed to passed to Chew's algorithm to triangulate.

For each vertex v , intersect each face incident upon v with a protecting circle of radius r centered at v . This could be viewed as forming a protecting sphere of radius r around v . We also install the edge-protectors. Consider an edge e . For every face incident upon e , we place a Steiner point on the protecting arcs of that face at both of the endpoints of e a distance d_e from e and form the parallel protecting edges as before by connecting these Steiner points. This can be imagined by intersecting a cylinder with radius d_e and axis e with the incident faces of e . We also place Steiner points at the orthogonal projection of these Steiner points onto e . As before, we do not consider the arcs on each face inside the edge protector; we consider the buffer-zone of a face to be anything inside the protecting circle or within a distance d_e of e on the face.

We now refine the boundaries of the buffer-zones. To do so, we compute a spacing value based upon the closest-pair of features that can arise. This is a function of the dihedral angles and the closest pair of Steiner points placed in the vertex and edge protection steps above. Specifically, let α be the smallest dihedral angle of P . Let d_f be the length of the base of an isosceles triangle with angle α and side lengths d_e . Compute an appropriate value for h using the arcs on the boundary of the buffer-zones and the lengths of the protecting edges, as in Section 2.2. Let $h' = \min(h, d_f)$. Note h' is less than or equal to the distance between any incident faces sharing an edge at a point outside the buffer-zone. We refine the arcs and the protecting edges for some value $h'' \leq h'$ chosen so that Chew's spacing requirements are satisfied. We must also ensure that the protecting edges are refined identically, as well as the edges they are protecting. We can now run Chew's algorithm on the portion of each face of P outside of the buffer-zones to create a conforming Delaunay triangulation with h'' as the maximum radius.

We claim that every one of Chew's triangles satisfies Lemma 2. Why? First, the circumradii of Chew's triangles not incident upon an edge of the buffer-zone do not intersect any other entity in the PLC, due to the bounds on the circumradii. Second, if a circumradius of one of Chew's triangles intersects another face, it is because it is incident upon the buffer-zone. We claim it only intersects a portion of a buffer-zone where no points are placed. This follows from the alignment of Steiner points of the protecting edges and the input edges and the bounds on the circumradii. It is straightforward to show the points inside the buffer-zones do not interfere with each other; their minimum diameter circumspheres cannot intersect because of the spherical and cylindrical distributions, point alignment on the edges and edge-protectors, and edge spacing. This gives our main result:

THEOREM 3.1. *A PLC P can be refined so that the Delaunay tetrahedralization of its augmented vertex set conforms to P with a finite number of Steiner points.*

4 Conclusion

In essence, we have given a generalization of Saalfeld's Conforming Delaunay triangulation algorithm to three dimensions. Like its planar counterpart, our algorithm places far too many points to be practical and should be viewed more as an existence proof. Thus, it would be interesting to know if an algorithm that runs in polynomial time based on the input size (and therefore places a polynomial number of Steiner points) exists, akin to the two-dimensional result in [ET93]. It would also be interesting to find a Conforming Delaunay tetrahedralization algorithm sensitive to the local-feature-size that could be coupled with standard "quality" measures of tetrahedra with general PLCs. Algorithms to compute Conforming Delaunay simplicial complexes of PLCs in higher dimensions would also be of interest.

References

- [Bak99] T. Baker. Delaunay-Voronoi methods. In J. F. Thompson, B.K. Soni, and N.P. Weatherill, editors, *Handbook of Grid Generation*, pages 16.1–16.11. CRC Press, Boca Raton, 1999.
- [BE92] M. Bern and D. Eppstein. Mesh generation and optimal triangulation. In D.-Z. Du and F. K. Hwang, editors, *Computing in Euclidean Geometry*, volume 1 of *Lecture Notes Series on Computing*, pages 23–90. World Scientific, Singapore, 1992.
- [BP97] M. Bern and P. Plassmann. Mesh generation. *Unpublished Manuscript*, 1997. Available at <http://www.ics.uci.edu/~eppstein/280g>.
- [CDE⁺99] S.W. Cheng, T.K. Dey, H. Edelsbrunner, M.A. Facello, and S.H. Teng. Sliver exudation. In *Proc. 15th Annu. ACM Sympos. Comput. Geom.*, 1999.
- [Che89a] L. P. Chew. Constrained Delaunay triangulations. *Algorithmica*, 4:97–108, 1989.
- [Che89b] L. P. Chew. Guaranteed-quality triangular meshes. Technical Report TR 89-983, Dept. Comput. Sci., Cornell Univ., Ithaca, NY, 1989.
- [CM99] P.R. Cavalcanti and U.T. Mello. Three-dimensional constrained Delaunay triangulation: A minimalist approach. In *Proc. 8th International Meshing Roundtable*, Albuquerque, NM, 1999. Sandia National Laboratories.
- [ET93] H. Edelsbrunner and T.-S. Tan. An upper bound for conforming Delaunay triangulations. *Discrete Comput. Geom.*, 10(2):197–213, 1993.
- [GB98] P.L. George and H. Borouchaki. *Delaunay Triangulation and Meshing: Application to Finite-Elements*. Hermes, New York, NY, 1998.
- [Geo99] P.L. George. Tet meshing: Construction, optimization, and adaptation. In *Proc. 8th International Meshing Roundtable*, Albuquerque, NM, 1999. Sandia National Laboratories.
- [HKM95] M. Held, J.T. Kłowsowki, and J.S.B. Mitchell. Evaluation of collision detection methods for virtual reality fly-throughs. In C. Gold and J.-M. Robert, editors, *Proc. 7th Canad. Conf. Computat. Geometry*, pages 205–210, 1995.
- [Law77] C. L. Lawson. Software for C^1 surface interpolation. In J. R. Rice, editor, *Math. Software III*, pages 161–194, New York, NY, 1977. Academic Press.
- [MTT⁺96] G.L. Miller, D. Talmor, S.-H. Teng, N. Walkington, and H. Wang. Control volume meshes using sphere packing: Generation, refinement, and coarsening. In *Proc. 5th International Meshing Roundtable*, Albuquerque, NM, 1996. Sandia National Laboratories.
- [PS85] F. P. Preparata and M. I. Shamos. *Computational Geometry: An Introduction*. Springer-Verlag, New York, NY, 1985.
- [Rup95] J. Ruppert. A Delaunay refinement algorithm for quality 2-dimensional mesh generation. *Journal of Algorithms*, 18(3):548–585, 1995.
- [Saa91] A. Saalfeld. Delaunay edge refinements. In *Proc. 3rd Canadian Conf. Comp. Geometry*, pages 33–36, 1991.
- [SF73] G.J. Strang and G. Fix. *An Analysis of the Finite-Element Method*. Prentice-Hall, 1973.

- [She97] J. R. Shewchuk. *Delaunay refinement mesh generation*. PhD thesis, School of Computer Science, Carnegie Mellon University, 1997. Available at <http://www.cs.berkeley.edu/~jrs>.
- [She98a] J. R. Shewchuk. A condition guaranteeing the existence of higher-dimensional constrained Delaunay triangulations. In *Proc. 14th Annu. ACM Sympos. Comput. Geom.*, 1998.
- [She98b] J. R. Shewchuk. Tetrahedral mesh generation by Delaunay refinement. In *Proc. 14th Annu. ACM Sympos. Comput. Geom.*, 1998.
- [Wei87] K. J. Weiler. The radial edge structure: A topological representation for non-manifold geometric modeling. In J. Encarnacao M. Wozny, H. McLaughlin, editor, *Geometric Modeling for CAD Applications*. Springer Verlag, 1987.